

Silver-Bismuth Bimetallic Functionalized Negative Electrode for Iron-Chromium Flow Battery

Runze Li^a, Yang Guo^b, Han Yan^a, Shiling Yuan^{a,b}, Meng Lin^{a,*}

^aSchool of Chemistry and Chemical Engineering, Shandong University, Jinan 250100, P. R. China.

^bSchool of Chemical Engineering, Shandong Institute of Petroleum and Chemical Technology, Dongying 257061, P. R. China.

*Corresponding authors: (M. Lin) mlin@sdu.edu.cn

Experimental section

1. Material and reagents

Graphite felt (GF) was purchased from Liaoning Jingu Carbon Material Co., Ltd. L-(+)-tartaric acid ($\text{C}_4\text{H}_6\text{O}_6$, $\geq 99.5\%$) and bismuth nitrate pentahydrate ($\text{Bi}(\text{NO}_3)_3 \cdot 5\text{H}_2\text{O}$, $\geq 98.0\%$) were purchased from Shanghai Aladdin Biochemical Technology Co. Silver nitrate (AgNO_3 , AR), Hydrochloric acid (HCl , 36-38%) and nitric acid (HNO_3 , 65-68%) were purchased from Sinopharm Chemical Reagent Ltd. Ferrous chloride tetrahydrate ($\text{FeCl}_2 \cdot 4\text{H}_2\text{O}$, 98%) and chromium trichloride hexahydrate ($\text{CrCl}_3 \cdot 6\text{H}_2\text{O}$, AR) were purchased from Shanghai Macklin Biochemical Technology Ltd.

2. Preparation of silver-bismuth composite modified electrode

Firstly, the GF needs to be ultrasonicated in anhydrous ethanol and deionized water in turn for 30 min to clean the surface impurities, after which the GF is dried in a drying oven at 100°C . Subsequently, the GF was placed in a muffle furnace at 400°C for 5 h to obtain thermal graphite felts (TGF). A three-electrode system (TGF for the working electrode, a platinum foil electrode for the counter electrode, and a saturated calomel electrode for the reference electrode) was used to electrodeposit at a constant voltage of -0.6 V (vs. SCE) for 100 s to obtain the silver-bismuth composite modified electrode. The AgBi-TGF (Ag:Bi@1:3) was prepared from electrodeposition solution containing 0.06 M $\text{Bi}(\text{NO}_3)_3 \cdot 5\text{H}_2\text{O}$, 0.02 M AgNO_3 , 0.03 M $\text{C}_4\text{H}_6\text{O}_6$ and 5 M HNO_3 .

To further investigate the role played by silver-bismuth elements in the electrode reaction, the following samples were prepared using the same method and electrodeposition solutions with different silver-bismuth ion concentrations: (i) 0.06 M $\text{Bi}(\text{NO}_3)_3 \cdot 5\text{H}_2\text{O}$ (Bi-TGF), (ii) 0.06 M AgNO_3 (Ag-TGF), (iii) 0.06 M $\text{Bi}(\text{NO}_3)_3 \cdot 5\text{H}_2\text{O}$, 0.06 M AgNO_3 (Ag:Bi@1:1), (iv) 0.06 M $\text{Bi}(\text{NO}_3)_3 \cdot 5\text{H}_2\text{O}$, 0.01 M AgNO_3 (Ag:Bi@1:6)

3. Characterization

The morphological features of the samples were investigated using scanning electron microscopy (SEM, Thermo Fisher Quattro S, USA). Elemental distribution was analyzed via energy-dispersive X-ray spectroscopy (EDS) mapping. Surface chemical composition and valence states were characterized by X-ray photoelectron spectroscopy (XPS, Thermo Scientific ESCALAB 250Xi, USA). Crystalline structure analysis was performed using X-ray diffraction (XRD, Rigaku Ultima IV, Japan) with $\text{Cu K}\alpha$ radiation. Hydrophilicity assessment was conducted through static contact angle measurements using a goniometer (KRUS DSA25B, German), with the testing solution containing 1 M $\text{FeCl}_2 \cdot 4\text{H}_2\text{O}$, 1 M $\text{CrCl}_3 \cdot 6\text{H}_2\text{O}$, and 3 M HCl.

4. Electrochemical performance evaluation

Electrochemical evaluations were conducted using a CHI750E electrochemical workstation (Chenhua Instruments, China) with a three-electrode system comprising the modified working electrode, a saturated calomel reference electrode (SCE), and a platinum foil counter electrode. Cyclic voltammetry (CV) measurements were performed in an electrolyte containing 1 M $\text{FeCl}_2 \cdot 4\text{H}_2\text{O}$, 1 M $\text{CrCl}_3 \cdot 6\text{H}_2\text{O}$, and 3 M HCl across a potential window of -0.8 to 0 V (vs. SCE) at a 10 mV/s scan rate. Linear sweep voltammetry (LSV) was subsequently carried out in 3 M HCl solution, scanning from 0 to -1 V (vs. SCE) at an ultra-low rate of 1 mV/s. Electrochemical impedance spectroscopy (EIS) was implemented in the same mixed Fe/Cr electrolyte as CV, applying a 5 mV AC amplitude superimposed on a -0.2 V DC bias (vs. SCE) over a frequency range of 0.1 Hz to 100 kHz.

5. Single cell performance

The electrochemical performance of ICFB (Hefei Cogent Materials Technology

Co., Ltd., China) was evaluated using the battery test system (VRFB-CTP, Hefei Cogent Materials Technology Co., Ltd., China) with three distinct electrode configurations. All cells employed 3 cm × 3 cm GF as positive electrodes, while negative electrodes varied across groups - Group 1 (GF), Group 2 (TGF), and Group 3 (AgBi-TGF). The cells were assembled with 6.0 cm × 6.0 cm Nafion 115 membranes (DuPont, U.S.A.) and filled with 50 mL electrolyte per reservoir containing 1 M $\text{FeCl}_2 \cdot 4\text{H}_2\text{O}$, 1 M $\text{CrCl}_3 \cdot 6\text{H}_2\text{O}$, and 3 M HCl. A stepped current density protocol was implemented with four consecutive charge/discharge cycles at each increment from 40 to 80 mA/cm² (10 mA/cm² intervals), followed by a cycling stability assessment through 100 charge/discharge cycles at fixed 60 mA/cm² current density.

Results and discussion

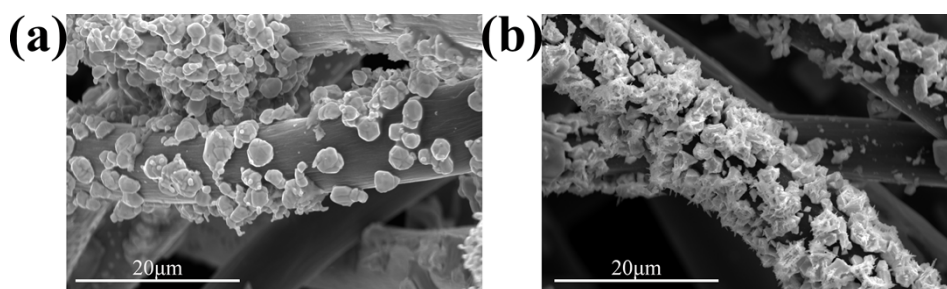


Fig. S1. (a) SEM image of Ag-TGF. (b) SEM image of Bi-TGF.

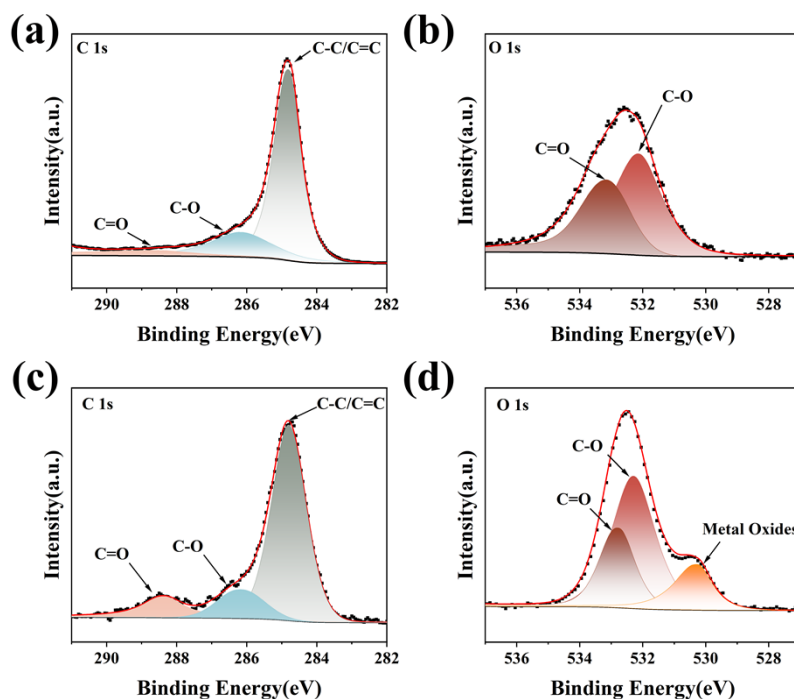


Fig. S2. (a) C 1s, (b) O 1s XPS spectra of the TGF. (c) C 1s, (d) O 1s XPS spectra of

the AgBi-TGF.

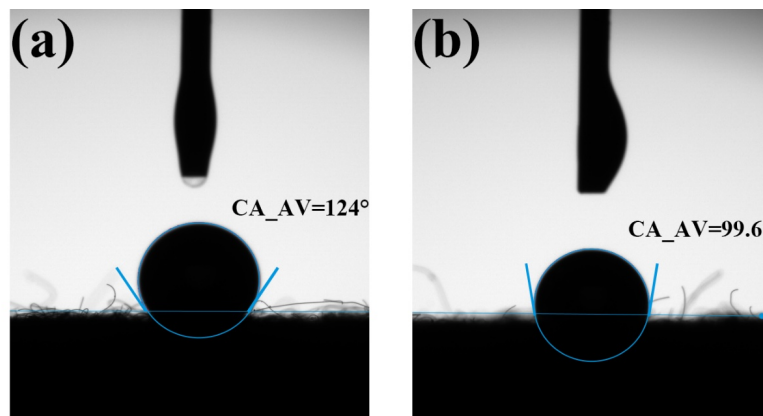


Fig. S3. Contact angle measurements for (a) the GF and (b) the AgBi-TGF.

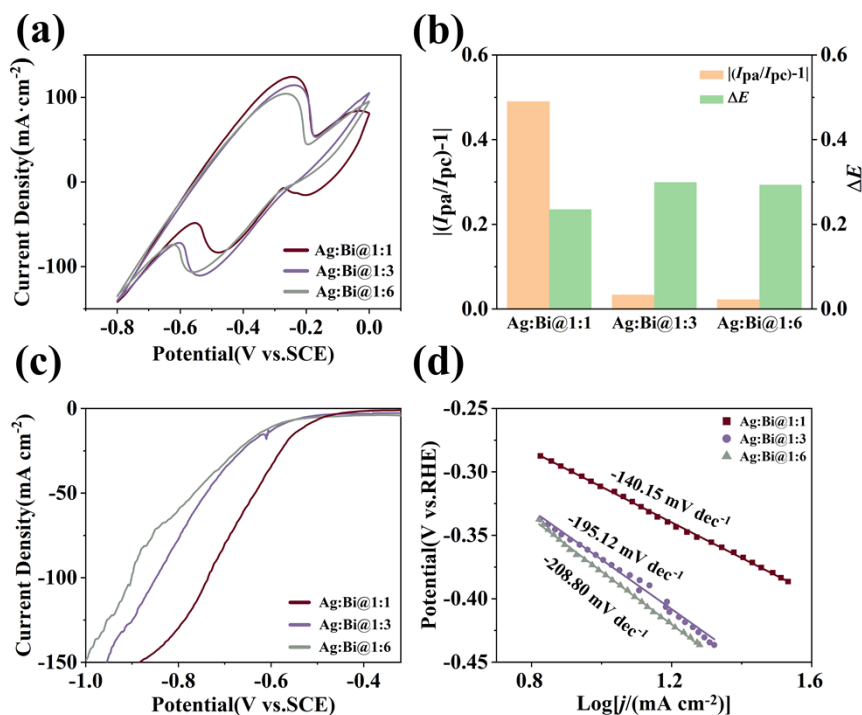


Fig. S4. (a) CV curves of $\text{Cr}^{3+}/\text{Cr}^{2+}$ on different samples. (b) The potential difference at the peak current and peak current ratio statistics for different samples. (c) LSV curves of $\text{Cr}^{3+}/\text{Cr}^{2+}$ on different samples. (d) Tafel plots of $\text{Cr}^{3+}/\text{Cr}^{2+}$ on different samples.

This study systematically evaluated the electrochemical performance of three silver-bismuth ion ratios (Ag:Bi@1:1, 1:3, 1:6) in electrodeposition solutions to determine the optimal composition. As shown in Fig. S4, the evaluation system focuses

on three key parameters, reaction intensity, electrochemical reversibility, and hydrogen evolution reaction (HER) suppression capability. For oxidation/reduction reaction intensity (Fig. S4a), Ag:Bi@1:1 exhibits the strongest oxidation activity but the weakest reduction performance, while Ag:Bi@1:6 shows insufficient oxidation intensity. Ag:Bi@1:3 demonstrates the most balanced redox characteristics. Electrochemical reversibility analysis (Fig. S4b) reveals that Ag:Bi@1:6 achieved the best reversibility metrics (smallest ΔE and $|I_{pa}/I_{pc}-1|$ closest to 1), with Ag:Bi@1:3 following closely.^{1,2} Ag:Bi@1:1 displays the poorest reversibility due to its significantly deviated current ratio ($|I_{pa}/I_{pc}-1|$). HER inhibition capacity tests are shown in Fig. S1c-d, that a smaller absolute value of the Tafel slope corresponds to stronger HER activity.³ Ag:Bi@1:1 initiates HER at -0.5 V (vs. SCE) with the worst Tafel slope ($-140.15 \text{ mV} \cdot \text{dec}^{-1}$). Ag:Bi@1:6 exhibits a delayed HER onset potential (-0.55 V) and Tafel slope is $-202.80 \text{ mV} \cdot \text{dec}^{-1}$, while Ag:Bi@1:3 demonstrates intermediate HER suppression performance between these two ratios, yet shows significantly better inhibition capability compared to Ag:Bi@1:1 ($-195.12 \text{ mV} \cdot \text{dec}^{-1}$). Moreover, compared to Ag:Bi@1:6, its higher silver content enhanced the binding strength of bismuth on the electrode surface. Based on this multi-parameter optimization, Ag:Bi@1:3 was selected as the optimal composite-modified electrode composition for subsequent comparative experiments.⁴

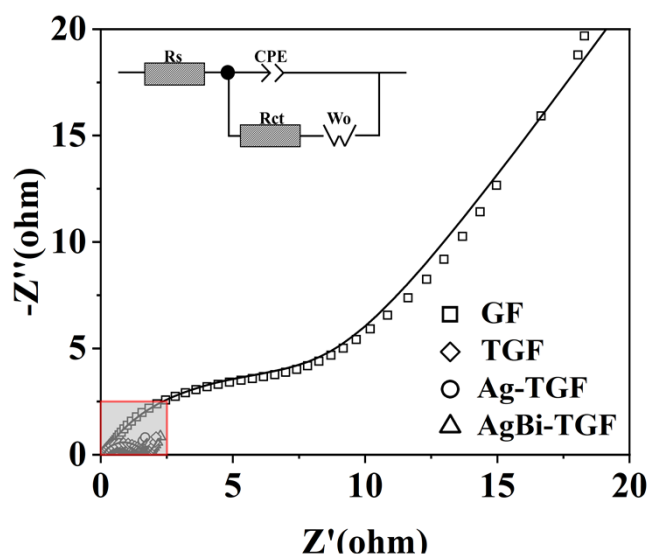


Fig. S5. Nyquist plots of $\text{Cr}^{3+}/\text{Cr}^{2+}$ on different samples.

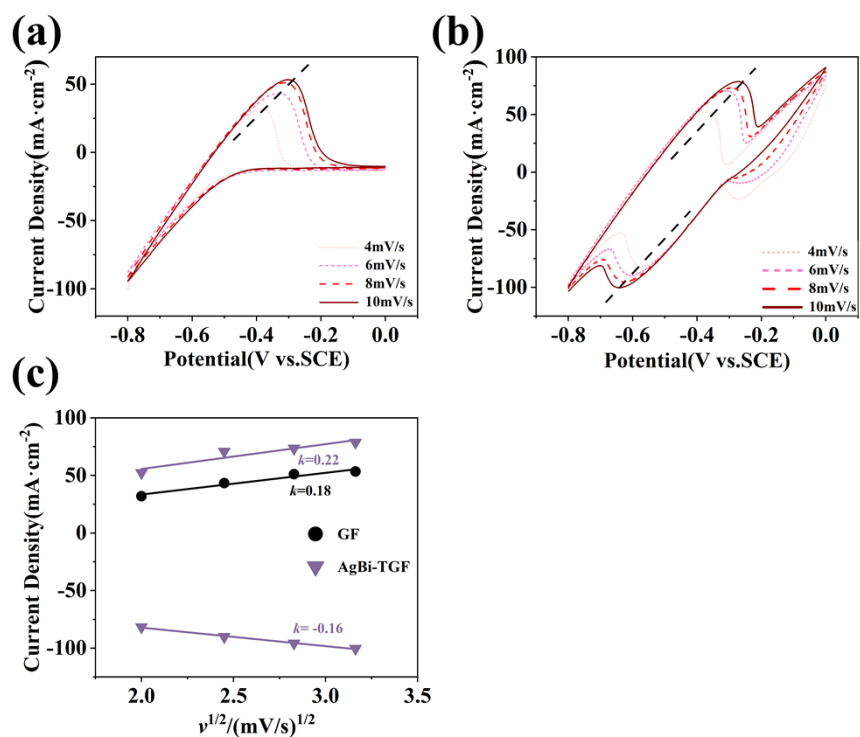


Fig. S6. Different scanning rates of (a) the GF (b) the AgBi-TGF. (c) Calculated diffusivity for $\text{Cr}^{3+}/\text{Cr}^{2+}$ couple.

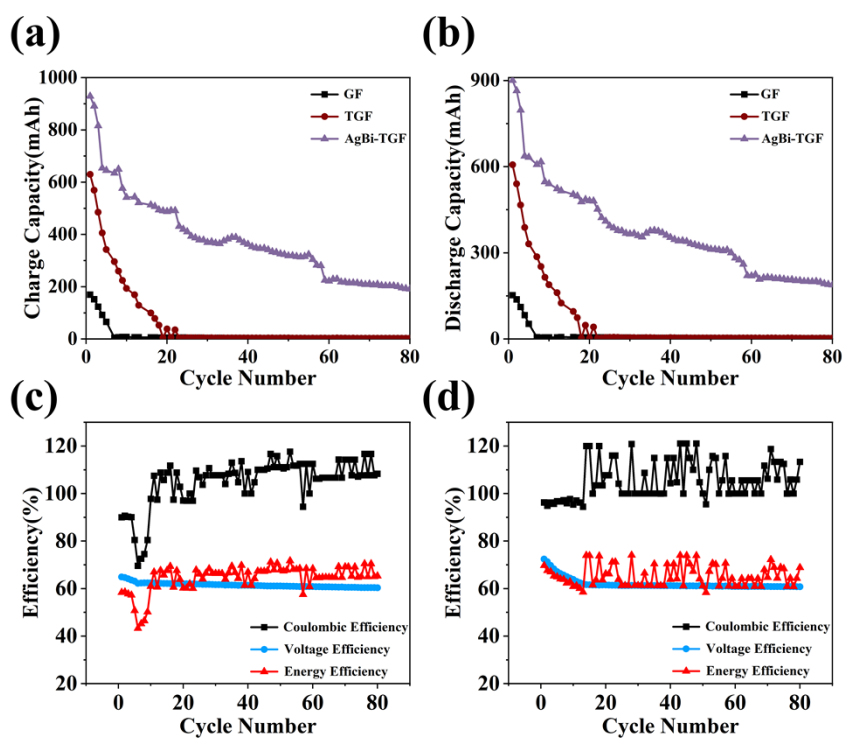


Fig. S7. (a) Charge and (b) discharge capacity curve after 80 cycles at 60 mA/cm² of different samples. CE, VE and EE after 80 cycles at 60 mA/cm² of (c) the GF and (d) the TGF.

Table S1. Atomic % of GF and AgBi-TGF.

Sample	C	O	Ag	Bi
GF	70.08%	9.61%	-	-
AgBi-TGF	45.17%	43.60%	5.24%	5.99%

Table S2. Redox parameters of different modified electrode obtained from CV curves.

Sample	$-E_{pa}(V)$	$-E_{pc}(V)$	$I_{pa}(mA/cm^2)$	$I_{pc}(mA/cm^2)$	I_{pa}/I_{pc}	ΔE
GF	0.343	/	26.52	/	/	/
TGF	0.309	/	66.33	/	/	/
Ag-TGF	0.148	/	111.29	/	/	/
Bi-TGF	0.315	0.561	78.36	123.33	0.635	0.246
AgBi-TGF	0.244	0.479	124.27	83.42	1.490	0.235

Table S3. Numerical statistics of impedance of fitted circuits.

Sample	R_s	R_{ct}	CPE		W_o		
			$Y_0/\Omega^{-1}\cdot s^n$	n	R_o	W_o-T	W_o-P
GF	0.11836	6.001	0.0017034	0.77697	9.509	0.12	0.33235
TGF	0.11322	1.488	0.0002322	0.83706	0.727	1.37	0.36441
Ag-TGF	0.11451	0.765	0.0001083	0.86201	0.935	1.73	0.30817
AgBi-TGF	0.10701	1.234	0.0003291	0.93257	0.670	1.29	0.35056

References

1. Q. Li, J. Liu, A. Bai, P. Li, J. Li, X. Zhang, M. Yu, J. Wang and H. Sun, *J. Chem.*, 2019, **2019**, 8958946.
2. C. Xie, H. Yan, Y. Song, Y. Song, C. Yan and A. Tang, *J. Power Sources*, 2023, **564**, 232860.

3. O. van der Heijden, S. Park, R. E. Vos, J. J. J. Eggebeen and M. T. M. Koper, *ACS Energy Lett.*, 2024, **9**, 1871-1879.
4. Y. Liu, Y. Niu, C. Guo, F. Qu, Z. Liu, X. Zhou, W. Guo, C. Xu and Q. Xu, *Energy Fuels*, 2024, **38**, 12202-12211.